0618

RD&E

CENTER

Technical Report

No. 13204

By Donald McIntyre and Eberhard A. Meinecke

U.S. ARMY TANK-AUTOMOTIVE COMMAND
RESEARCH, DEVELOPMENT & ENGINEERING CENTER
Warren, Michigan 48397-5000

XX(4571.1)

NOTICES

This report is not to be construed as an official Department of the Army position.

Mention of any trade names or manufacturers in this report shall not be construed as an official indorsement or approval of such products or companies by the U.S. Government.

Destroy this report when it is no longer needed. Do not return it to the originator.

REPORT DOCUMENTATION PAGE

1a. REPORT SECURITY CLASSIFICATION Unclassified	1b. RESTRICTIVE MARKINGS None
2a. SECURITY CLASSIFICATION AUTHORITY	3. DISTRIBUTION/AVAILABILITY OF REPORT Approved for public release: Distribution is unlimited
2b. DECLASSIFICATION/DOWNGRADING SCHEDULE	
4. PERFORMING ORGANIZATION REPORT NUMBER(S)	5. MONITORING ORGANIZATION REPORT NUMBER(S) 13204
6a. NAME OF PERFORMING ORGANIZATION Institute Polymer Science University of Akron 6b. OFFICE SYMBOL (If applicable)	7a. NAME OF MONITORING ORGANIZATION U.S. Army Tank-Automotive Command
6c. ADDRESS (City, State, and ZIP Code) Akron, OH 44325	7b. ADDRESS (City, State, and ZIP Code) Warren, MI 48397-5000
8a. NAME OF FUNDING/SPONSORING ORGANIZATION TACOM 8b. OFFICE SYMBOL (If applicable)	9. PROCUREMENT INSTRUMENT IDENTIFICATION NUMBER DAAE07-83-C-4011
8c. ADDRESS (City, State, and ZIP Code) ATTN: AMSTA-RCKT Warren, MI 48397-5000	10 SOURCE OF FUNDING NUMBERS PROGRAM ELEMENT NO. / PROJECT NO. / TASK NO. / WORK UNIT ACCESSION NO.

11. TITLE (Include Security Classification)
Elastomer Suitable for Track Pad Use that will Change from the Amorphous to the Crystalline State on Stress Application (UNCLASSIFIED)

12 PERSONAL AUTHOR(S) Donald McIntyre and Eberhard A. Meinecke

13a. TYPE OF REPORT	13b. TIME COVERED	14. DATE OF REPORT (Year, Month, Day)	15. PAGE COUNT
Final	FROM 12/82 TO 5/86	6/8/86	55

16 SUPPLEMENTARY NOTATION

17. COSATI CODES			18. SUBJECT TERMS (Continue on reverse if necessary and identify by block number)
FIELD	GROUP	SUB-GROUP	Rubber blends, natural rubber, SBR, high temperature behavior (of natural rubbers), crystallization, microgel, (continued on reverse side)

19. ABSTRACT (Continue on reverse if necessary and identify by block number)

(1) Novel blends of model elastomers were synthesized to determine their potential use in tank track pads to be used at high temperatures, pressures and shearing stresses. (2) The effect of strain-induced crystallization, microgel inclusions, and reinforcing gelled filler on the physical properties of elastomers was determined. (3) The physical and chemical properties of natural rubber at track pad temperatures and of styrene butadiene rubber (SBR) under cyclic deformation superimposed on compression similar to track pad conditions was determined.
(continued on reverse side)

20. DISTRIBUTION/AVAILABILITY OF ABSTRACT	21. ABSTRACT SECURITY CLASSIFICATION	
☒ UNCLASSIFIED/UNLIMITED ☐ SAME AS RPT. ☐ DTIC USERS	Unclassified	
22a. NAME OF RESPONSIBLE INDIVIDUAL Jacob Patt	22b. TELEPHONE (Include Area Code)	22c. OFFICE SYMBOL AMSTA-RTT

DD FORM 1473, 84 MAR 83 APR edition may be used until exhausted. All other editions are obsolete.

Block 18 continued.

entanglements, heat build-up (in rubber), degradation of natural rubber, crystalline/amorphous blends

Block 19 continued.

(1) The strain induced crystallization of compatible blends of cis-1,4 polyisoprene and trans 1,4 polyisoprene shows an improvement of mechanical properties before vulcanization compared to pure cis 1,4 polyisoprene, but the final properties of the vulcanized blends are not improved. Related studies with cis and high vinyl polybutadiene show similar studies with cis and high vinyl polybutadiene show similar behavior. The effect of molecular weight and crystal type of the blended polymer indicate that only chemically bonded blends of crystalline/amorphous polymers can bring about improved properties in the vulcanized state.

(2) The effect of microgel on the homogeneity of crosslinks in vulcanized and unvulcanized rubber was determined. The natural rubber microgel was found to increase the ultimate properties of natural rubber. When the microgel adheres to the reinforcing filler, the ultimate elongation can be increased by 40%. A loop theory of entanglement was developed to explain the observed phenomena of strain-induced crystallization and the effect of microgel on flow properties.

(3) The number of effective entanglements in natural rubber at temperatures from 90°C to 125°C was determined by both stress relaxation and gel permeation chromatography so that an effective mechanical equation of state could be formulated from the activation energy of 95 kJ/mol. The degradation of natural rubber above 125°C was studied in detail by combined mass-spectrometry and thermal analysis. The chemical fragments, kinetic parameters and effect of impurities are given.

The heat build-up in bonded SBR rubber blocks while undergoing cyclic stresses with applied static deformations of (i) extension and (ii) compression was measured. The thermal properties of the rubbers (specific heat and thermal diffusivity) were measured as a function of carbon black loading and compared with prediction from a finite difference method.

TABLE OF CONTENTS

TABLE OF CONTENTS (Continued)

LIST OF ILLUSTRATIONS

LIST OF TABLES

1.0. INTRODUCTION

During the past three years the University of Akron Institute of Polymer Science has done extensive experimental and theoretical work to improve and understand the strain-induced crystallization (SIC) of elastomers for tank-pad use, working under contract DAAE07-83-R011. To this end, new elastomers and new elastomer blends have been made and evaluated. Also commonly used tank pads of natural rubber (NR) and styrene-butadiene rubber (SBR) have been examined under high stresses and high temperatures to discover how these materials mechanically and chemically behave under modern track pad use.

2.0. OBJECTIVES

The research objective was to increase the performance of track pads by increasing the strength of rubbers through strain-induced-crystallization using both natural rubber and other model elastomers. For this purpose, methods of measuring stress crystallization were to be developed and also new rubbers and rubber blends were to be synthesized for testing. Systematic experimental studies of the effect of crystalline additives and gel additives on the strength of rubers, both at ambient temperatures and at operating temperatures were to be correlated and explained.

3.0. CONCLUSIONS

Five major conclusions have been reached in the course of this work:

- Strain-induced crystallization can be improved in the uncured state by blending NR with long-chain compatible crystalline compounds. However, in the cured state, the large increase in SIC is lost. Similar but ongoing studies on polybutadiene blends show the same increase in SIC with a long chain crystalline additive. Triblock elastomers with crystallizable segments show the same mechanical behavior, but being self-cured, they do not lose the SIC.

- Strain induced crystallization can be increased in the uncured state by the addition of microgel. The addition of other small heterogeneities of plant tissue bound by microgel can also delay the onset of SIC.

- A model attributing the improved mechanical properties in SIC to increased loop entanglements of polymer chains caused by crystals or microgels has been proposed.

- New and precise measurements from 90°C to 200°C of the degradation of chain-length of NR suggest the loss of such entanglements and crosslinks under track pad operation -- and thus a dramatic change in the mechanical equation of state for the high temperature of operation.

- Dynamic studies of SBR under shear cycling were made to determine heat build-up as a function of carbon black bonding. Also the dynamic properties of SBR under static extension and static compression were measured and explained.

Each of these major conclusions is amplified briefly in the following sections with reference to the detailed data and calculations given in the appropriate thesis or other publication.

4.0. RECOMMENDATIONS

4.1. Studies under Track Pad Conditions

In the present work the study of two track pad materials has been made under temperatures and stress conditions that approximate those of track pad operations, namely temperatures above 100° C and cyclic stress under compression. In these preliminary studies the chemical degradation of natural rubber was examined from 90° C to 180° C. Then in a series of parallel experiments the mechanical properties of SBR were measured under compression.

A similar study of both a model and an actual track-pad elastomer should be undertaken simultaneously to determine a valid thermo-mechanical equation of state for comparison with actual temperatures and stress profiles of the same track pad material. Obviously SBR, NR, or some other better performing single or blended elastomer ought to be studied in this light.

4.2. Evaluation of Fabrication Procedures in Light of New Theoretical and Experimental Results

The existing commercial method of fabricating track pads ought to be examined to determine if a change of procedures can enhance the homogeneity of track pads, purposely enhance fracture resistance or avoid deterioration of properties under high temperatures and cyclic shear compression. The present

work has given both a theoretical model and two practical examples in which the role of micro-gell and small gelled reinforcing particles can drastically affect the ultimate elongation and SIC of natural rubber materials.

The effect of added micro-gells and gelled reinforcing particles on the extrusion or molding of track pads material should be studied to determine the feasibility of producing more homogeneous track pads or building in specifically designed heterogeneities to enhance the final track pad performance. New lab scale processing using new ideas of the loop entanglement theory might lead to much better track pads than current conventional practices.

4.3. Investigation of New Materials

The search for new elastomers or new blends of existing elastomers with unique properties should be explored in a rational manner. The physical properties in the unvulcanized state are enhanced by crystallites that enhance stress-induced crystallization, yet in the vulcanized state there is little real enhancement. However, when the crystallites are chemically tied-down to the amorphous chain the physical properties of the blend continue to stay enhanced. Thus blends (or blocks) involving small amounts of a stable high temperature crystalline polymer ought to be further explored to determine the optimal conditions for such reactions. Experiments in filled and unfilled systems should be done.

5.0. DISCUSSION

5.1. Blending Crystalline Materials with Elastomers to Increase Strain-Induced Crystallization

5.1.1. Blends with Natural Rubber

5.1.1.1. Properties of vulcanized cis- and trans-polyisoprene blends. Elastomers are routinely blended with other polymers to improve their physical and mechanical properties. These polymers may be either another elastomer having some special properties or a crystalline or amorphous plastic. The physical properties of some elastomer-plastic blends and blocks under study are reported elsewhere[1]. The mechanism by which the second polymer improves the physical properties in the compatible or incompatible blends is not clear.

A few factors that influence the blended elastomer properties are: (a) the thermodynamic compatibility that controls the

phase separation and domain size, (b) the viscosity of the elastomer blend that controls the diffusion of one polymer into another, (c) the molecular weight of the polymer that controls domain interfaces, and (d) the distribution of additives that affects their function. These considerations have been reviewed by Corish[2]. To understand the enhancement of properties in blends, it is desirable to eliminate systematically the many complicated, interacting factors by starting with a compatible ideal system. Few such fundamental studies on elastomer blends have been reported although a few detailed investigations have been reported on homopolymeric blends of isotactic and atactic polystyrene[3].

Compatible homo-elastomer blends have gained increasing attention in recent years. Ubepol VCR, a polybutadiene (BR) having a high cis-BR combined with 10% of syndiotactic 1,2 BR, has a high modulus, high hardness, high cut growth resistance, good tear resistance, small mill shrinkage, small die swell, and excellent processability[4]. The relation of elastomeric micro- and macro-structure to the properties of compounded rubber is also not well established. A preliminary study has been reported by Corish[5]. A tire tread compound with solution polymerized styrene-butadiene copolymers that have a relatively high 1,2 butadiene content has been designed to reduce the rolling resistance of tires and improve wet grip[6]. Similar studies relating micro-structure to compound properties have been reported recently[7].

Among all these blends, a mixture of cis- and trans-polyisoprene (c-PI and t-PI) would seem to be ideal for fundamental studies in the sense that the glass transition temperatures are comparable, the melting points of the crystals are close, and the experiments can be easily performed above and below the melting point. Cooper and Vaughan[8] measured the crystallization of blends of NR and t-PI by differential thermal analysis and by dilatometry. They reported that a mixture of NR and t-PI causes a marked reduction in the rate of crystallization of NR in the unstretched state. More recently, Thomas et al.[9] found a single glass transition temperature at all compositions for same blends. All the blends showed spherulites, and the spherulitic growth rate decreased with the increase in non-crystallizable content. The lamellar crystal thickness changes only slowly with crystallinity. However, little is known about the following factors:

(a) the thermodynamic compatibility of these blends,
(b) the mechanical properties of these blends above and below the melting point of the crystal, and
(c) the stress induced crystallization of these blends.

These factors have been investigated in this work.

Blends of guayule rubber (GR) and t-PI have been investigated in order to understand the thermodynamic compatibility, technological properties, stress-strain isotherms at high elongation, birefringence and wide angle x-ray diffraction on stretched and unstretched rubber. Experiments have been performed at temperatures above and below the melting point of t-PI. Both crosslinked and uncrosslinked systems have been used. Blends of GR and t-PI at all compositions show complete thermodynamic compatibility.

The technological properties of all these blends using a tire tread recipe without fillers indicate that the blends at a higher percentage (20%) of t-PI lose most of their rubber properties and that the t-PI does not co-crystallize on stretching with the c-PI. Tensile strength at high temperature is, however, increased with the incorporation of t-PI. Stress-strain isotherms at high elongation show that the critical value of λ at which upturn occurs (λ_c) decreases with increase in t-PI.

Wide angle x-ray scattering experiments indicate that t-PI does not act as nucleating site for crystallization of c-PI. A new ring appears at 6.61 Angstroms on stretching for all the systems studied, and becomes more intense with higher values of λ. Measurements of birefringence also suggest that t-PI hinders the crystallization of GR. The stress optical coefficient decreases at room temperature with an increase in t-PI indicating that t-PI acts more like an inert filler. The stress optical coefficient, however, increases at an experimental temperature above the melting point of t-PI crystals. With ten parts of t-PI in the blend most of the physical properties measured do not show any abrupt change.[10]

5.1.1.2. SIC of unvulcanized blended c-PI and t-PI. A mixture of c-PI and t-PI was used in this study because the glass transition temperatures are comparable, the melting points of the crystals are close, and the experiments can be easily performed above and below the melting point. Kuo[11] studied these blends by differential scanning calorimetry (DSC) and reported that these polymers are thermodynamically compatible. More recently, Bhowmick et al.[12] reported technological, optical and elastic properties of stretched vulcanized mechanical blends above and below the melting points of the crystal.

Simultaneous measurements were made of stress and birefringence on unvulcanized solution blends of Hevea rubber (HR) SMR-5 (Standard Malaysian Rubber, dirt < .5%), c-PI, and synthetic t-PI (Weight average molecular weight (Mw) = 3.21 x 10^5), uniaxially stretched to high elongations.

Stress and birefringence followed power law decays. The rates of birefringence relaxation and stress relaxation decrease with elongation and t-PI content. The rates of stress relaxation are higher than the rates of birefringence relaxation for the blends here studied. Stress-strain and birefringence-strain plots exhibit the drastic increase typical of SIC at high elongation. The elongation at which the SIC phenomenon initiates decreases with t-PI content.[13]

5.1.1.3. Strain-Induced Crystallization of Natural Rubber Blended with Crystallites of Large and Small Molecules. Attempts were made to improve strain-induced crystallization of NR by adding small amounts of external nucleating agents. A variety of organic substances (acids, paraffins, low molecular weight (MW) crystals and polymers) having suitable crystallographic properties were used.

Several criteria were used to select the 22 organic crystals listed in Table 5-1. Materials were chosen having unit cell parameters equivalent, greater or smaller than c-PI (a = 12.4 Å, b = 8.9 Å, c = 8.15 Å) and representing the six crystal systems. Melting points (MP), MW, unit cell volumes, and densities are given for each of the materials listed in Table 5-1.

The effect of the foreign particles was investigated by measuring the stress-strain curves at room temperature and at 70°C and comparing the results to those obtained for pure NR. The curves were sorted into three groups depending on the behavior of the curve relative to the standard (S) as shown in the Figure 5-1. The stress-strain curves corresponding closely to NR (within+-10%) are labelled same, S. Curves with true stress exceeding NR by more than 10% (at equal extension ratios) are labelled better, B. Those curves with stress more than 10% less than NR are labelled worse, W.

The experimental results are divided in the following groups: 1) mechanical blends with low MW crystals, 2) mechanical blends with polymeric materials, 3) solution blends with low MW crystals and, 4) solution blends with polymeric materials.

The stress-strain behavior of mechanical blends with low MW crystals at room temperature is summarized in Table 5-2. Three of the four blends whose curves are in the W region (Table 5-2.) have the common property that the melting temperature of the pure crystals is greater than the temperature of preparation (urea MP = 132°C, tartaric acid MP = 173°C, Anthracene MP = 214°C). However, this is not the general rule because the hexamethylene-tetramine (MP = 270°C) average curve is in the S region. The other blend in the W region is

Table 5-1. Crystallographic Parameters of Small Molecules Used in Blends

NAME	MOL WT (g/mol)	M.P. °C	CRYSTALLOGRAPHIC DATA a	b	c	α	β	γ	Vol	Form	DENSITY (g/ml)
A. Urea	60.06	132.4	5.63		4.70				149.0	Tetragonal	1.3230
E. Naphthalene	128.17	80.2	8.235	8.080	6.003		115° 55′		359.3	Monoclinic	1.152
F. Hexamethylene-tetramine	140.19	290	7.03						347.4	Cubic	1.331
I. Biphenyl	154.21	69	9.57	5.67	8.11		94° 30′		438.7	Monoclinic	.992
K. Acenaphthene	152.21	93	8.3	14.2	7.26				855.7	Orthorhombic	1.0242
D. Anthracene	178.23	214	9.439	6.036	8.561		103° 31′		474.2	Monoclinic	1.283
J. Azobenzene	182.23	68	15.19	5.71	12.20		112° 36′		987.1	Monoclinic	1.203
H. Bibenzyl	182.27	52	11.67	6.12	7.70		100° 22′		541.0	Monoclinic	1.014
M. Iodoform	393.73	122	6.81		7.524				302.2	Hexagonal	
C. Oxalic acid	126.07	102	11.88	3.60	6.12		103.5°		254.5	Monoclinic	1.64
B. Tartaric acid	150.09	173	7.72	6.0	6.2		100° 17′		282.6	Monoclinic	1.7598
L. Lauric acid	200.32	44	27.62	4.965	9.524		96° 55′		1296.6	Monoclinic	0.8679
G. Stearic acid	284.49	69	43.99	7.39	5.68		93° 26′		1843.2	Monoclinic	0.9408
PA. Octadecane	254.51	29	4.820	23.07	4.285	92° 4′	107° 18′	91° 6′	454.4	Triclinic	0.7768
PB. Tetracosane	338.66	50	7.42	31.25	5.35	95° 6′	99°	90° 42′	1220.0	Triclinic	.7991
PC. Octacosane	394.77	61									.8067
PD. Dotricontane	450.89	70									.8124
TP. trans-Polyisoprene	$1.67*10^5$	64	7.84	11.87	4.75				442.0	Orthorhombic	
"	$2.56*10^5$	64									
"	$3.21*10^5$	64									
"	$6.53*10^5$	64									
"	$11.94*10^5$	64									

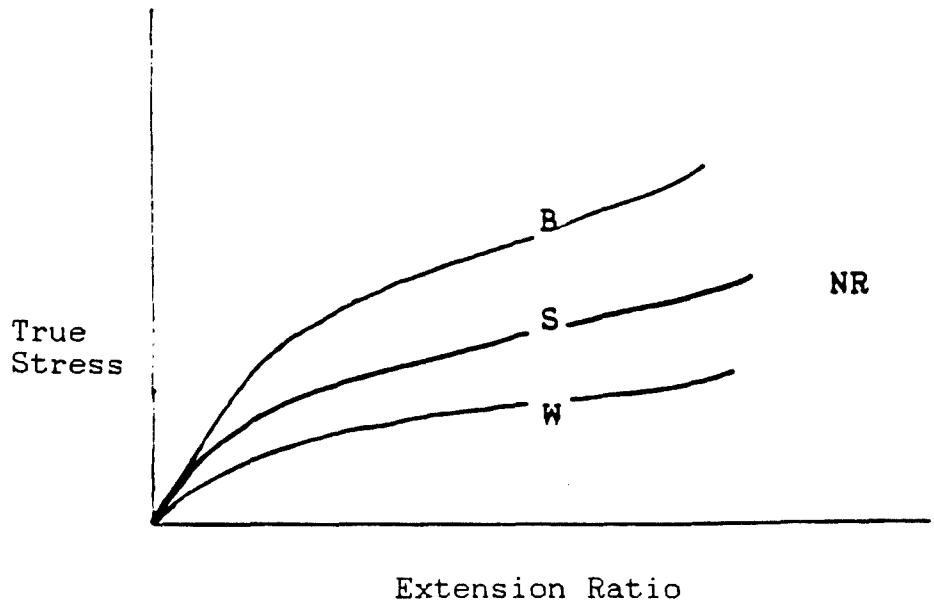

Figure 5-1. Behavior of the Stress-Strain Plots.

Table 5-2. Relative Properties of Blends Studied

		Region	E_r	λ_r	$(F\lambda A_o^{-1})_r$
T.	Hevea rubber	S	1.0	1.0	1.0
A.	Urea	W	1.0	1.1	1.0
E.	Naphthalene	B	1.0	0.7	0.8
F.	Hexamethylene tetramine	S	1.0	0.8	0.7
I.	Biphenyl	S	0.9	0.9	0.9
K.	Acenaphthene	S	1.7	0.8	0.8
D.	Anthracene	W	0.8	0.9	0.7
J.	Azobenzene	S	1.2	0.8	0.8
H.	Bibenzyl	S	0.8	1.0	1.0
M.	Iodoform	S	1.7	0.6	0.5
C.	Oxalic acid	S	0.9	0.5	0.6
B.	Tartaric acid	W	0.8	0.7	0.7
L.	Lauric acid	S	0.8	0.8	0.8
G.	Stearic acid	B	1.2	1.0	1.2
PA.	Octadecane	W	0.9	0.8	0.7
PB.	Tetracosane	S	0.9	1.0	0.9
PC.	Octacosane	S	1.0	1.2	1.2
PD.	Dotricontane	B	1.1	1.4	1.7
TP.	trans-Polyisoprene				
	$1.67*10^5$	B	1.8	1.0	2.0
	$2.56*10^5$	B	1.9	1.0	1.7
	$3.21*10^5$	B	2.2	0.9	1.3
	$6.53*10^5$	B	1.8	1.0	1.8
	$11.94*10^5$	B	2.3	0.8	1.0

octadecane (MP = 29°C). Blends with stearic acid, dotriacontane, and naphthalene are in the B region. The initial and final properties (initial slope or Young's Modulus, and true stress and extension ratio at rupture respectively) of the fatty acid and the paraffin blends are greater than those for NR. The final properties of the napthalene blends are less than those for NR.

In order to compare these curves in more detail, the relative initial slope and relative ultimate properties were used. The relative initial slope, E_r, is defined as the initial slope of the stress-strain curve relative to that of NR. Similarly, the relative final properties λ_r and $(f\lambda A_o^{-1})_r$ are defined for the strain ratio and stress at break. Table 5-2 shows these values. The blends with compounds having equal or similar molecular weight have similar initial and final mechanical properties. The final quantities increase with MW as is clearly seen for acids and paraffins. It is apparent that better results are obtained only for crystals with MW greater than ~250. The E_r values are so scattered that a clear tendency cannot be observed.

Plots of relative mechanical properties as a function of the melting point of the crystals show that these qualities are improved for some materials with 50°C < Temp (MP) < preparation temperature.

In order to investigate the effect of crystalline phase on the stress-strain results, experiments were performed at 70°C with blends of the same conposition as before. For a better direct comparison, experiments at room temperature were also repeated. The results show the same general aspects described above. With the exception of stearic acid and acenaphthene blends, the curves at high temperatures are in the W region. The crystals in the liquid state act as diluents, and decrease the values of true stress and final properties. At the 70°C temperature the stearic acid has just melted and does not modify the stress-strain curve of HR. For acenaphthene the behavior is the same at 70°C and room temperature.

The polymer used in the mechanical blends is t-PI with the following molecular weights measured by gel permeation chromatography (GPC):

Mw x 10^{-5}	Mw/Mn
1.67	1.3
2.56	1.3
3.21	5.3
6.53	1.6
11.94	1.4

At room temperature all the curves are in the B region and their shape is different from that of HR. Their slopes near $\lambda = 4$ increase abruptly, consequently having greater final stress values. It is clear from the plots of room temperature that the stress increases with the molecular weight of t-PI. The addition of t-PI may increase the entanglement of the molecular chains. However at high temperatures when t-PI has melted, the t-PI has the behavior of a diluent.

The plots of reduced stress vs λ^{-1} show a minimum or upturn at about $\lambda_c = 6$. This behavior may be ascribed to the finite extensibility of chains, and also to strain-induced crystallization. For experiments with pure HR in which the extension ratio at rupture is greater than this value, the upturn is not observed. This means that the effect of adding t-PI is to increase entanglements of the rubber chains and therefore reduce their extensibility. The observed values of λ_c are high and are taken near the rupture point elongation so that it is difficult to have a representative average. In addition, some blends did not show the upturn which is attributed to a possible lack of local homogeneity in the distribution of t-PI in the rubber matrix. The value of λc also depends on the t-PI content.

Solution blends with low MW crystals have been prepared with HR masticated at 70°C in the same way as the mechanical blends. The shape of the plots is similar to that found in the experiments with mechanical blends. However, there are some differences. In the solution blended experiments, the stresses and elongations are greater, and almost all the solution blended samples show a miminum in the reduced force curve. Only dotricontane and anthracene blends have curves in the B region. However, the two blends with curves in the B region for the mechanically blended samples were dotricontane and stearic acid.

The values for the relative initial slope are similar to those corresponding to mechanical blends. However, the values of the relative final properties are very low because the samples of pure HR broke at very high extension ratios ($\lambda = 14.5$) while the blends broke at about $\lambda = 9$.

In Figure 5-2 the behavior of the reduced force is shown as a function of λ^{-1} for single experiments with HR and for blends whose stress-strain curves are in the B or W regions. These curves have a minimum at $\lambda_c = 7\text{-}8$. An absence of this behavior is seen in mechanical blends with the same crystals. This may indicate that solution blended samples have more entanglements than mechanical blends.

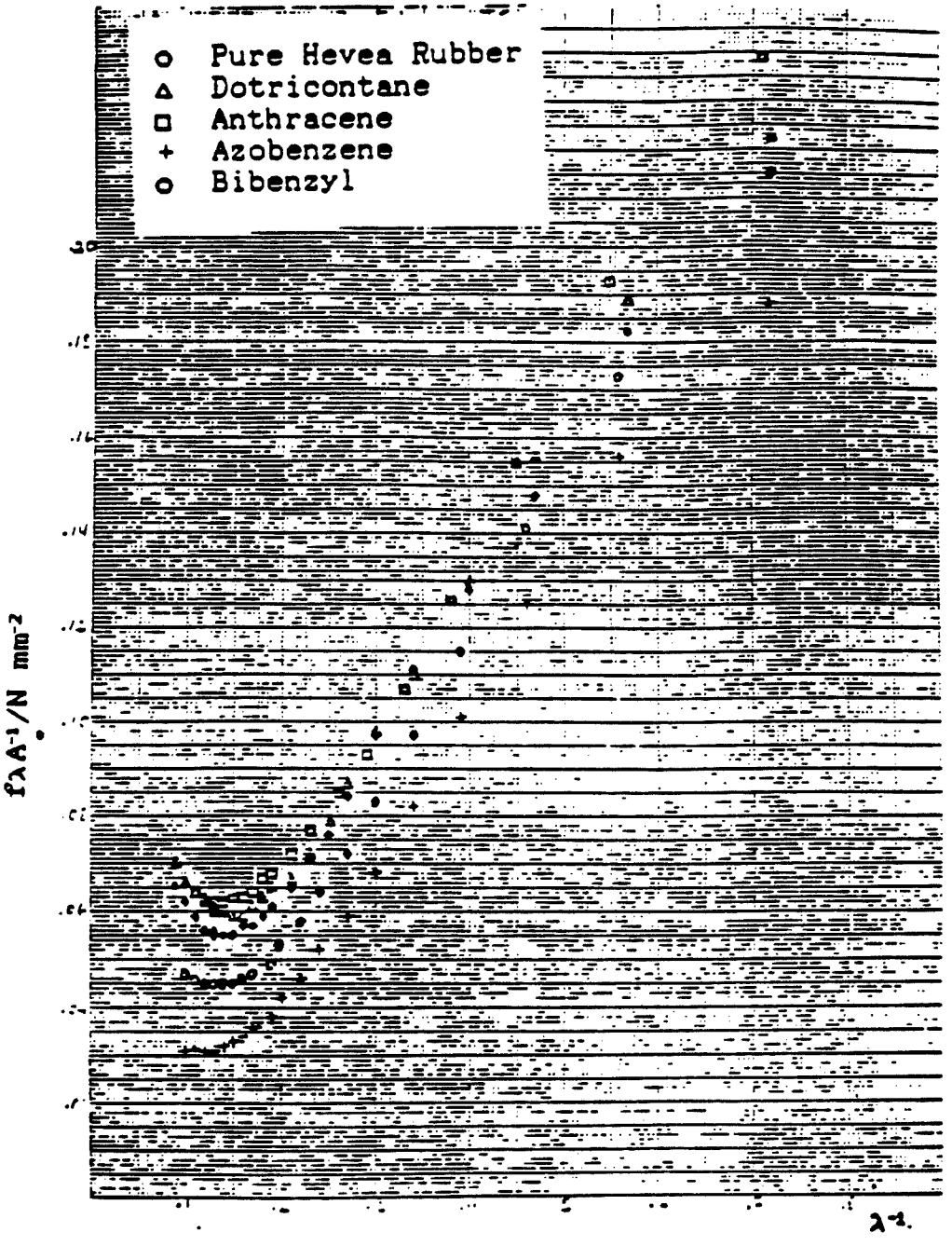

Figure 5-2. Reduced Stress vs. Extension Ratio for Solution Blends at Room Temperature

Gee has proposed an equation for the reduced force of rubber. Neglecting the effect of crystallization he obtained for crosslinked NR

$$[f] = g_2 + 1/2\ A_4 g_2^2(\lambda^2 + \lambda^{-2}) + 3A_0 g_2^{1/2}\ \ln\lambda(\lambda^2 - \lambda^{-1})^{-1}$$

$A_0 = 0.66$ and $A_4 = 0.82$, where [f] is in Nmm^{-2} and g_2 is an adjustable constant for each sample and is to a good approximation proportional to the crosslinking. Particularly satisfactory is the way in which the positions of the minima are represented.

Gee's equation has been applied to the neighborhood of the minimum of the reduced force shown by single experiments with solution blends of GR with t-PI in different proportions. The fitting is illustrated in Figure 5-3 for uncrosslinked and crosslinked samples. The crosslinked samples were at the same (gamma) radiation exposure. The stress-strain results of these crosslinked blends were reported previously. The values of g_2 and the position of the minimum (λ_c^{-1}) increase with the t-PI content. One effect of t-PI in NR is to produce a blend that behaves qualitatively similar to a crosslinked rubber. That is, it increases the physical crosslinks or entanglements.

5.1.2. Blends with Elastomers Other Than Natural Rubber

5.1.2.1. Synthesis of new elastomers. The synthesis of experimental polymers is categorized into three general methods of polymerization: 1) high vacuum line, 2) bottle polymerization, and 3) batch reactor. Each method has advantages and disadvantages based on differing criteria. All were used in the synthesis of new elastomers for this work.

The new polymers made in bottles and the 1 gallon reactor were:

1) Homogeneous anionic polymerizations of:
   - isoprene
   - butadiene
   - p-methyl styrene
   - styrene

2) Ziegler-Nata polymerizations of:
   - cis and trans isoprene
   - cis and trans butadiene
   - piperylene (1,3 pentadiene)
   - myrcene (2 methyl-6-methylene-2,7 octadiene)

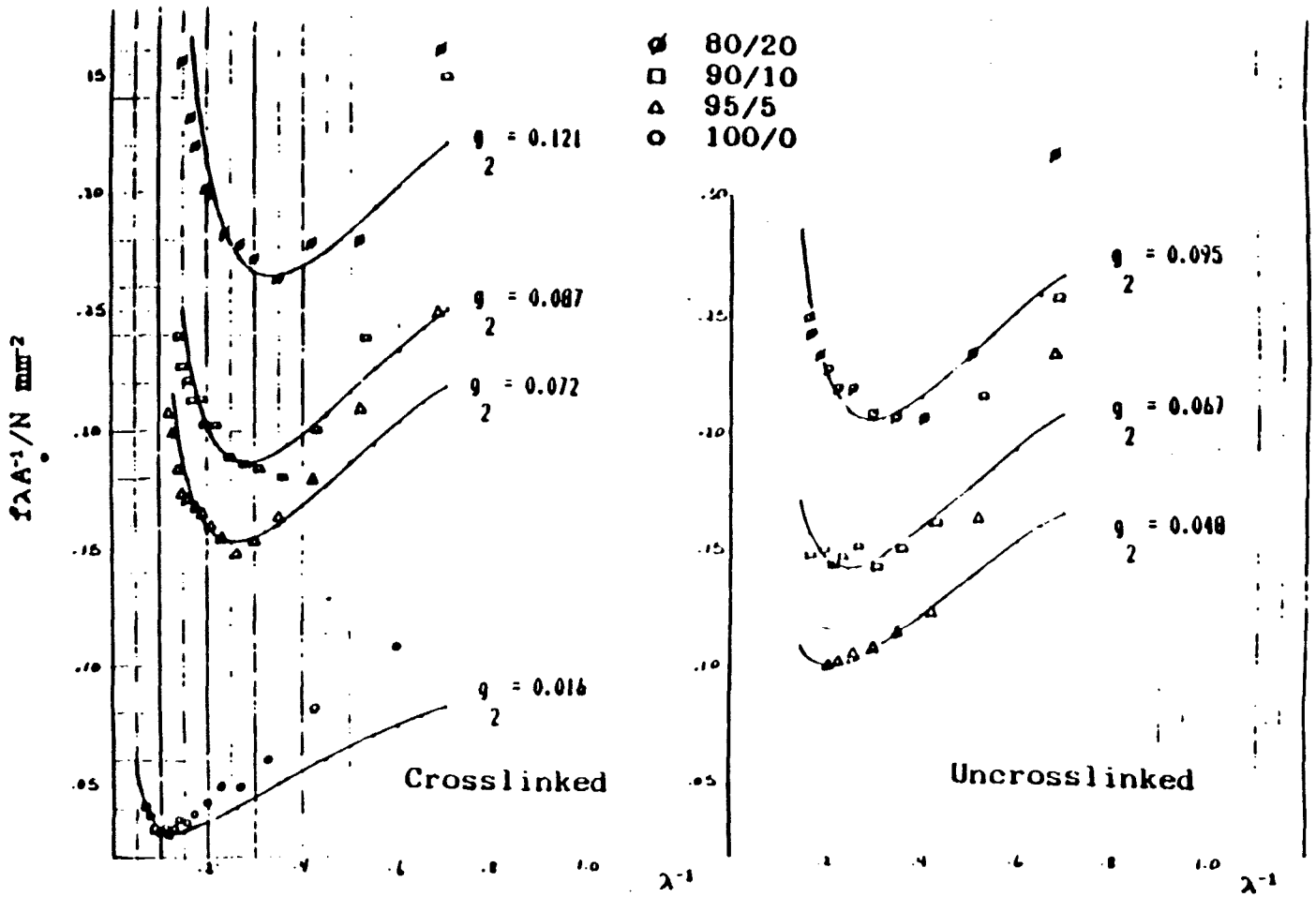

Figure 5-3. Reduced Stress vs. Extension Ratio for Solution Blends with t-PI at Room Temperature

3) block polymerizations:
   - diblock anionic butadiene isoprene
   - Ziegler-Natta crossover dienes

4) ring opening:
   - i-5 cyclooctadiene

5.1.2.2. Strain Induced Crystallization of Poly(butadienes). This section summarizes studies of the effects of adding crystalline homopolymers to a strain crystallizable, highly stereoregular cis-1,4-polybutadiene (cis-BD). The crystalline polymers used were stereoregular isomers of polybutadiene, namely, trans-1,4 (trans-BD) and syndiotactic 1,2-PBD (vinyl-BD). Stereoregular cis-BD readily strain crystallizes at room temperature, as shown by a new diffraction ring in wide angle x-ray scattering (WAXS), the presence of deformed spherulitic scattering patterns by low angle laser light scattering (LALLS), and optical density changes in samples extended to about 400%. Hence, these studies concerned the effects a deliberately added crystalline component may have in such a crystallizable matrix as cis-BD.

Blend compatibility influences material properties. A crystallizing, compatible blend should show maxima in most mechanical properties. DSC studies indicate that blends of trans with cis-BD are probably compatible, whereas blends of vinyl and cis-BD are definitely incompatible.

Blends with trans-BD were judged 'probably compatible' on the basis of melting point depressions of the blends, and decreasing trans-BD spherulite size with increasing volume fraction cis-BD. Stress-strain isotherm measurements indicate a crystallization process to occur at extensions of around 350-450%. The process is dependant on volume fraction trans-BD used, up to about 15% (w/w). LLALS data indicate a second type of solid scattering from these blends, probably from ordered regions of small crystallites, at high extensions. Optical density measurements suggest the addition of trans-BD affects the extent and rate of cis-BD crystallization. Time dependant studies show the blend crystallizes by a growth of rodlike crystals from an instantaneous nucleation mechanism, consistent with theories of strain-induced crystallization.

Blends with vinyl-BD were judged incompatible on the melting point and LLALS bases. A commercial blend used, Ubepol VCR (vinyl cis rubber), containing 12% vinyl-BD, has good mechanical properties. Unfortunately, varying the vinyl-BD content proved very difficult, due to the insolubility and high melting point (202°C) of the vinyl-BD. Nevertheless, the limited blends available showed a moderate change in

crystallization based on composition. Stress-strain isotherms indicate a small decrease in the critical extension required to induce crystallization when vinyl-BD is added. The enhancement of mechanical properties of these blends was judged to be due to an inert filling effect of the vinyl-BD, in addition to this polymer's fibrous nature providing a barrier to crack propagation. LLALS studies on deformed blend samples show a fiber deformation process to be the main stress releasing mechanism. Diffuse scattering probably due to some limited amorphous phase crystallization under stress was also found. Optical density data indicate that vinyl-BD has little influence on enhancing strain crystallization of cis-BD.

Compatible cis/trans-BD blends affect the crystallization of the cis-BD matrix. The largest effect in modifying cis-BD crystallization is seen in those blends with low added crystal content. Generally, 1-5% (w/w) of added crystalline polymer works best. Blends with vinyl-BD show mainly the inert filler nature of the vinyl polymer imbedded in a cis matrix.

5.2. Blending Microgel with Elastomers to Increase Strain Induced Crystallization

5.2.1. Crystallization and Strain Birefringence of Uncrosslinked Natural Rubber as a Function of Molecular Weight and Gel Content. One of the outstanding properties of natural rubber is its crystallizability by freezing or by stretching. The presence of crystalline sites improves the physical properties of rubber. The S-shape in stress-strain curves and the relaxation process are related to the crystallization character. the crystallization of rubber is affected by many factors: temperature, pressure, chemical composition, amd molecular weight. In this study rubber fractions with varying molecular weight and gel content were prepared through the fractionation of natural rubber. The fractions were then subjected to freezing and elongation at room temperature. The crystallization during these processes was characterized by DSC measurements and birefringence measurements.

The different amounts of crystallization with and without stress were attributed to the differing amounts of entanglement in natural rubber that hinders crystal growth. Since higher molecular weights have much more entanglement, and since gels enhance the entanglement, the fractions containing differing amounts of each were examined to determine the limiting percent crystallinity or chain orientation.

DSC measurements show that with an increase in the freezing time, the crystallinity increases for all samples. At similar

molecular weight, the sample with higher gel content gives lower crystallinity. A 7% increase in crystallinity is observed by reducing the gel content by one-fourth.

Stress-relaxation measurements show that the sample with higher gel content always has a higher modulus. A similar effect was also observed with changes in molecular weight. The gel and high molecular weight have a stiffening effect on the relaxation modulus and these reduce the rate of relaxation markedly. The enhancement of mechanical properties with the incorporation of gel is probably due to (1) the higher modulus of the gels, because these gels are chemically entangled systems and (2) the complete compatibility of these particles with the matrix.

The effect of gel on the stress-strain curve is very similar to that of t-PI in rubber. At a similar gel level, the higher molecular weight sample shows superior stress-strain properties to the lower molecular weight samples. The effect of gel is more dominant on the stress-strain properties than the effect of molecular weight.

Birefringence decreases with time for samples stretched at low elongation, but it increases with time at higher elongations. Gel particles are acting as crosslinks and resist the flow of non-crystrallized molecules after stretching.

The details of these measurements are given in the M. S. thesis of Jeongmi Cho, University of Akron, 1985, entitled "Crystallization and Strain Birefringence of Uncrosslinked Natural Rubber as a Function of Molecular Weight and Gel Content."[14]

5.2.2. Residual Plant Tissues from Guayule Rubber Processing and Their Effect on Failure Properties of Natural Rubber. Guayule rubber, obtained from guayule shrubs (*Parthenium argentatum*) grown in the southwestern part of the United States is an alternative source of natural rubber. Baled shrubs are treated with hot water to remove earth and leaves. The defoliated shrubs are then pased through both a hammer mill and a Bauer mill to break open the rubber-filled cells. The spongy mass known as "worms" is collected and passed through a series of flotation tanks to remove bagasse. The worms are then extracted with acetone to remove resins. The deresinated rubber is then purified by dissolution in hexane and filtration to remove the residual insolubles like cork, fiber, and dirt. The above process (or any alternative process) for obtaining guayule rubber must contend with some unwanted non-rubber ingredients in the rubber of which residual plant tissue is dominant.

These plant tissues are termed "dirt" and may lower the physical properties and quality of the rubber. There is, of course, no standard definition of dirt; but there is general agreement that significant amounts of dirt particles are deleterious to the high performance of natural rubber. Unlike carefully harvested and processed HR, dirt cannot be avoided in GR. It is therefore necessary to know the amount of dirt that can be tolerated in the rubber without impairing its technological properties.

Greensmith[15] studied the effect of sand and sawdust on the strength of HR. He found a non-linear dependence of failure properties on particle concentration. At high concentrations, only a portion of the dirt acted as flaws and the remainder acted as a diluent. Additionally, dirt had a greater effect on the fatigue properties than on the tensile strength. The coarsest particles were the most deleterious, but particles less than 45 αm in size had little effect on strength. Bateman[16] also observed that the tensile strength, tear strength and abrasion resistance were affected by large particles of sand. However, the nature of the dirt in HR is different from the dirt in GR which comes mainly from plant tissue. The effect of guayule dirt on the mechanical properties of rubber vulcanizates has not yet been studied.

Plant tissues are a non-rubber constituent of GR, like proteins in HR. The nature and morphology of the residual plant tissues may influence the properties. In this study, the residual plant material or dirt has been characterized in detail both alone and dispersed in HR. Also, a systematic study has been carried out to investigate the effect of dirt on the tensile and fatigue life of a simple vulcanizate of HR. The chemical structure of GR and HR are the same.[17]

Three of the grades of commercially available NR are SMR-5, SMR-20, and SMR-50, having maximum dirt specifications of 0.05%, 0.2%, and 0.5% dirt respectively. The physical properties of HR vulcanizates containing these levels of dirt were investigated.

"Dirt in HR[18] and GR has been classified into two groups: (1) those particles retained on a 325 mesh size sieve (45 αm), or "coarse" dirt, and (2) those particles that passed through the 325 mesh sieve, or "fine" dirt. A 325 mesh sieve has been specified the SMR scheme for the determination of the dirt content.

The residual plant tissues and minerals, termed here dirt, in GR have been characterized by microscopy, thermogravimetric analysis and chemical analysis. Their effect on the failure

properties of HR SMR-5, SMR-20, and SMR-50 has also been investigated.

The guayule plant tissues (dirt) have been classified and used as two arbitrary groupings: fine dirt with particle size less than 45 μm and coarse dirt with particle size greater than 45 μm. Both categories of dirt contain guayule rubber and minerals, but they are principally woody tisssue. Thermogravimetric analyses show 30-40% inorganic matter in the dirt. The inorganic matter consists of calcium, magnesium, iron, sodium, copper, and silica in varying proportions. The level of residual copper is within the specification for international standards of natural rubber. The dirt has a porous structure.

The addition of even .05% of coarse dirt is detrimental to tensile strengths (30% decrease) and fatigue to failure properties (40-50% decrease). However, vulcanizates with fine dirt even up to a level of 3% are comparable to samples with no dirt in the above properties. The decrease in these properties with coarse dirt is due to the fact that the dirt particles act as flaws in the matrix. The theoretical relation between stress at break or failure life under dynamic conditions and flaw size can correctly correlate all of the results.

Details of these measurements are given in two theses titled "The Effect of Residual Plant Tissue and Minerals on the Properties of Natural Rubbers"[19] and "Characterization of Guayule Plant Residues and their Effect Upon the Mechanical Properties of Rubber."[20]

5.3. Loops as an Equilibrium Topology for Very Long Strands and Applications to Polymer Properties

Tangling in macroscopic systems has been observed and was found in general to be unknotted. Tangling of long flexible strands was found to occur by means of interlocking loops. A form of analysis based on loop concepts has been developed and extended to the dynamic tangling behavior of moving strands. This loop analysis offers insight into many aspects of polymer behavior.

A method is developed for describing the interactions of discrete loops. This method leads to a concept of loop rank that is useful for understanding large multi-strand systems. An extension of this concept to a system of mobile loops gives an equilibrium distribution of loop ranks in a structure resembling random three dimensional knitting with many dropped stitches. Since entanglement by this model is a property of the entire system, it is not localized at "points of

entanglement" and the concept of "distance between entanglements" is not relevant.

The model developed in the course of this study appears to be consistant, both in method of formation and in structure, with observations of entanglement in random tangles formed spontanously in long macroscopic flexible strands. The concepts developed can be applied to a number of polymer problems and are useful in understanding polymer behavior, both in bulk and in solution in a wide variety of situations.

5.3.1. Static Interactions of Separate Loops

5.3.1.1. The linking sequence describes interactions between distinct loops in a tangle and is useful for understanding the behavior of tangled systems. Figure 5-4 is the simplest example of a loop interaction and illustrates the way in which such systems resist deformation. Loop B cannot be removed by pulling on the standing parts, i.e., the strands that enter the matrix, unless loop A is first withdrawn. If a third loop, C, passes through loop A as shown in Figure 5-5, loop B is not free until loops C and A are removed in that order.

These interactions may be represented by the linking sequence digraph, a directed graph in which the vertices represent loops and an edge. $V_i \rightarrow V_j$, signifies that the loop represented by vertex V_i passes through or locks the loop represented by vertex V_j.

The adjacency matrix, J, for a linking sequence digraph of n vertices, is an n x n matrix whose elements, J(i,j) are 1 if an arrow goes from V_i to V_j and are zero otherwise. The ijth element of the nth power of an adjacency matrix, $J^n(i,j)$, is the number of paths of n steps or n+1 vertices going from V_i to V_j. If the digraph is finite and contains no cycles, each path must contain at most n-1 steps and all powers of the adjacency matrix greater than n-1 must be zero.

5.3.1.2. The Concept of Loop Rank. Define the rank of a loop to be the number of loops which must be successively withdrawn before the loop is free. The rank of a tangle is that of the highest rank loop in the tangle. The rank of the tangle is therefore the highest power of the adjacency matrix having one or more non-zero elements. The rank is independent of the number of separate strands involved. The loops participating in a given tangle may belong to the same strand or to different strands. Furthermore, twisting of the loops does not affect the rank of the entanglement. The strands continue on to another loop of the same tangle, another tangle, or other random behavior. Untangling must begin with a zero rank loop, and no loop can be withdrawn until it has become zero

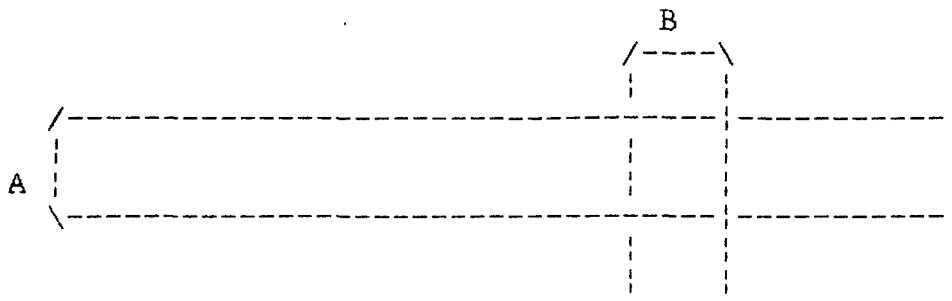

A → B

$$J = \begin{bmatrix} 0 & 1 \\ 0 & 0 \end{bmatrix} \qquad J^2 = 0$$

Figure 5-4. Loop A locks loop B and prevents it from moving downwards.

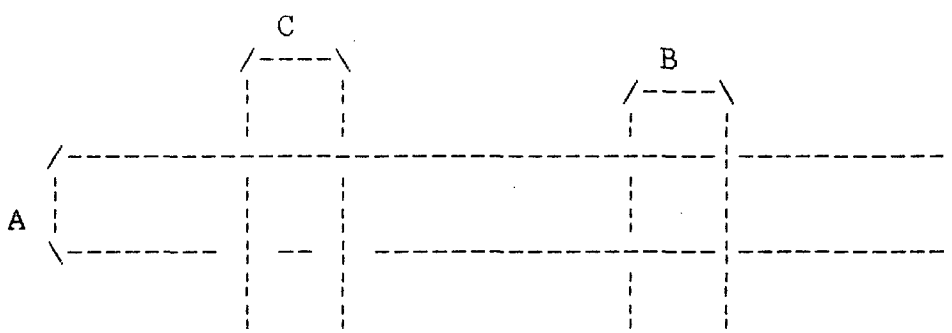

C → A → B

$$J = \begin{bmatrix} 0 & 1 & 0 \\ 0 & 0 & 0 \\ 1 & 0 & 0 \end{bmatrix} \qquad J^2 = \begin{bmatrix} 0 & 0 & 0 \\ 0 & 0 & 0 \\ 0 & 1 & 0 \end{bmatrix} \qquad J^3 = 0$$

Figure 5-5. Loop C now locks loop A, further restricting the motion of loop B. Both loops C and A must be removed before loop B is free.

rank by the removal of all loops passing through it. The addition of another zero rank loop increases the rank of the tangle only if it locks one of the zero rank loops that determine the rank of the tangle. The linking sequence of an unknotted tangle must have one or more zero rank loops. The column representing a zero rank loop in the adjacency matrix has no non-zero elements.

5.3.1.3. Dependence of Physical Properties on the Distribution of Loop Ranks. The distribution of loop ranks describes how interlocked the system is and may be expected to determine many properties of a elastomeric system above its glass transition. Loop rank can not be measured directly, and the precise dependence of properties on loop rank is not known at present. However it could be expected that better mechanical properties could be expected to result from an increase in the interlocking of the system, at least up to some optimum level. Further analysis and experiment are needed to identify the relevant variables and to clarify their interdependence.

5.3.2. An Unhindered System of Mobile Loops

5.3.2.1. Random Loop Interactions. A polymer above its glass transition is a system of flexible strands in constant random motion. Loops are constantly being thrust out and withdrawn and interactions of the type discussed above (in section 5.3) will occur to develop a structure resembling random three dimensional knitting with many dropped stitches. Above the level of entanglement needed to form a network, it is not necessary to distinguish between inter-molecular and intra-molecular interactions. As the loops move the rank of a given loop will change on a time scale that depends on the segmental jump frequency of the polymer. In a single step the rank of the loop may increase by one, decrease by one, or remain the same. Only the zero order loops of each sequence are active in the change in rank, and thus the probability of change can not depend on the rank of the sequence. The probability of a loop increasing, decreasing, or remaining the same in rank is independent of the rank of the loop except at zero rank and possibly at first rank. Therefore if the system is not under stress the rank of an individual loop forms a Markov chain with possible states 0, 1, 2, ..., and with a retaining barrier at 0. An equilibrium distribution exists for the system.

5.3.2.2. The Effect of Stress on a System of Mobile Loops. A zero rank loop placed under a stress perpendicular to the loop axis is extended and removed from the system. Extension of the sample is due to the response of the absorbed zero rank

loops within the cross-sectional area of the sample and can be calculated.

In an uncrosslinked system, untangling proceeds in this manner until the entanglement is insufficient to form a network. After that time the system consists of clusters of individual chains that are only tangled with members of the same cluster but are not tangled with chains of other clusters. The system can begin to flow at this time. The extension is then due both to untangling and to viscous flow in a system of decreasing cluster weight.

5.3.3. The Effect of Selective Immobilization of Some Loops of a Mobile System. This discussion applies to any type of selective immobilization of some loops of a tangled system. This immobilization can occur, for example, through chemical crosslinking, by attachment to a filler surface, by irregular or incomplete crystallization, or by locking of loops in an adjacent glassy domain. The precise effect of this immobilization will depend both on the location of the immobilized loops in the matrix, and also on the number of loops involved.

Unless it is specified otherwise, the distribution of the immobilized loops will be assumed to be random. The immobilization need not be permanent but must change on a time scale that is much slower than the step frequency of the Markov chain controlling the entanglement. In the calculations that follow, it is assumed that the system is at equilibrium before the immobilization. In the first discussion of crosslinking, the chemical reactions are assumed to be instantaneous and permanent. Later the effect of crosslink mobility and the rate of crosslinking will be discussed in section 5.3.4.2. below.

5.3.3.1. Notation of Crosslinks in the Linking Sequence Digraph. Crosslinks may be indicated on the linking sequence digraph by underlining the hindered loops. A crosslink at site 1 in Figure 5-6 will have no effect on this section of the entanglement. This may be written symbolically as A → A crosslink at site 2 in the same figure will prevent the removal of loop A and will thus prevent loop B from reaching zero rank. This interaction is written $\underline{A} \rightarrow B$. Loop B can, however, increase in rank by the passage of another loop through loop A as shown in Figure 5-7. This can be written $D \rightarrow \underline{A} \rightarrow B$. the probability that this will occur can be assumed to be unaffected by the crosslink at A.

5.3.3.2. Loop Dynamics in a Hindered System. The probability that loop B will increase in rank depends on the number of loops in the vicinity of loop A that are zero rank and

unhindered. The matrix of transition probabilities for a hindered system must therefore be decomposed into the weighted sum of a series of matrices with barriers at each rank, and with the weights of the matrices determined by the distribution of ranks at the instant of crosslinking.

5.3.3.3. Distribution of Loop Ranks in the Crosslinked System. The distribution of loop ranks in the crosslinked system can be calculated. The average rank of the hindered system depends on the average rank of the entanglement before it was crosslinked, as well as on the number of crosslinks. The average rank of the hindered system will therefore depend on the stress history of the material before crosslinking. Since the equilibrium average rank also depends on the temperature, the average rank after crosslinking will depend on the temperature at the time of crosslinking, and will be higher for lower temperatures. The results also imply that the properties of crosslinked and uncrosslinked rubber will differ more at high temperatures than at low temperatures because the change in maximum average rank is inversely proportional to the unhindered equilibrium rank, which is low at high temperatures. The temperatures considered are assumed to be above the glass transition temperature and below the temperature at which decomposition is a factor.

In some cases the hindrances to the loop motion are not permanent, but break and reform as a function of time. The shift in average rank will be time-dependent in this case and will approach a maximum that is higher than that obtained for the same number of permanent crosslinks formed simultaneously. This increase in average rank occurs because when a crosslink breaks and reforms after the entanglement has begun to move towards its post-crosslinking equilibrium, it interacts with a new distribution with higher average rank. It is clear from this argument that the effect of a given number of crosslinks will also depend on the rate at which they are introduced relative to the rate of change of the entanglement.

5.3.4. Applications. The topics in this section have been chosen to show the applicability of this model to a wide variety of polymer problems. The loop model requires no ends and is thus equally applicable to branched, cyclic, and lightly crosslinked polymers.

5.3.4.1. Creep and Stress Softening. When creep is calculated for an uncrosslinked system using this model, the curves are similar to those obtained by measuring creep in an uncrosslinked elastomer under constant load. A system of short chains flows immediately. As the number of loops is increased, a plateau develops that lengthens as the number of loops is increased further. Figure 5-8 shows the points

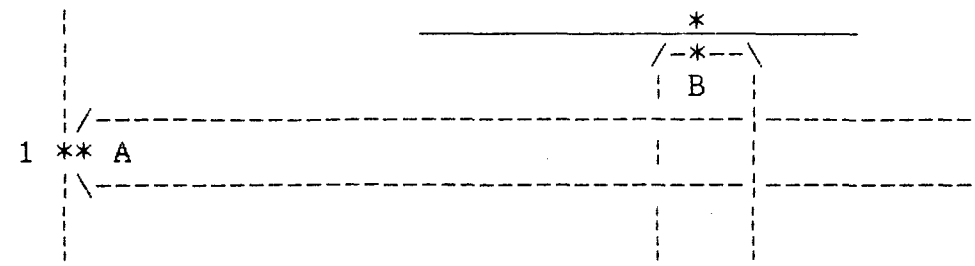

1. A → B

2. A → B

Figure 5-6. The untangling of this tangle is prevented by a crosslink at site 2 but not by one at site 1.

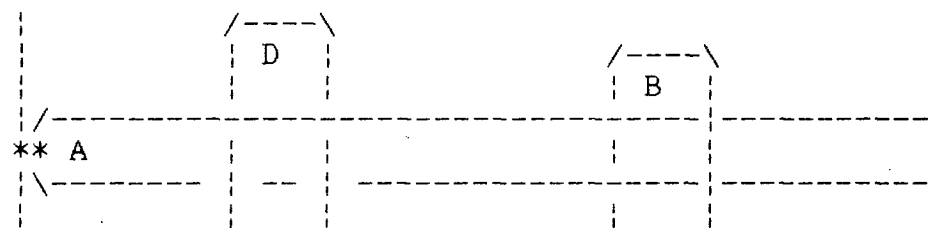

D → A → B

Figure 5-7. Further tangling of a hindered loop.

generated for five cases differing only in the number of loops.

When the tangled network is deformed, some of the zero rank loops are removed from the equilibrium by extension. Over the time that the stress is applied, more loops shift to zero rank and are extended. When the stress is removed, all the extended loops return to zero rank. If the stress is re-applied before the entanglement as been allowed to return to equilibrium, the number of zero rank loops available for immediate extension will be greater than the equilibrium number. This increase in zero rank loops allows the network to respond more readily up to the previous extension, where it will elongate as though it had not been previously stressed. This corresponds to the well-known phenomenon of stress softening.

5.3.4.2. Crosslinking. The discussion in section 5.3.3 describes the effect of crosslinks on the average rank of the entanglement. It is seen that crosslinks alter the probability of untangling some of the loops so that the equilibrium entanglement increases. The crosslinks do not enter directly into the load-bearing process and need only withstand the force of the random chain motions. The stress is carried at all times by the knitted structure of the entanglement. The creep behavior of crosslinked and uncrosslinked elastomers is similar through the plateau zone until the point where the uncrosslinked system begins to flow. The crosslinked system shows no sharp change in behavior but responds to an additional stress according to the superposition principle. This behavior suggests strongly that the extension is controlled in the same manner both in crosslinked and uncrosslinked systems.

When the average rank is calculated by the method described in section 5.3.3 and plotted against the length between crosslinks in arbitrary units, a curve is obtained that closely resembles that obtained when the tensile strength of natural rubber is plotted as a function of the molecular weight between crosslinks. These data support the hypothesis that the distribution of loop ranks influences the physical properties of the material. Figure 5-9 shows the calculated average rank plotted against the length between crosslinks.

The distribution of loop ranks in the crosslinked system depends on the distribution of ranks at the time of crosslinking and is therefore dependent on the thermal and stress history of the material prior to the crosslinking. The distribution of ranks is lowered by mixing or milling. A higher equilibrium average rank will be obtained after

processing if the compounded material is allowed to rest before vulcanization.

Because the average rank decreases as the temperature increases, an increase in rank can be maximized by minimizing the crosslinking temperature. Also, since the change in average rank due to the crosslinking is inversely proportional to the uncrosslinked equilibrium average rank at the measurement temperature, the mechanical properties of crosslinked and uncrosslinked rubber ought to differ more at high temperatures than at low temperatures. This behavior is of course observed.

The presence of small quantities of microgel can greatly enhance the properties of natural rubber. The calculation in section 4.3.4.2 assumed that the system was homogeneous and that the crosslinks were introduced randomly. Inhomogeneity will exist when microgel is introduced into the system and requires a more elaborate analysis. However, the enhancement in properties that occurs when small amounts of microgel are present in the system can be explained by the interaction of the unhindered loops of the uncrosslinked matrix interacting with the localized areas of higher crosslink density (and average rank) in the microgel over the large interface of the microgel.

5.3.4.3. Reinforcement. Reinforcement in this model arises from the interaction between inelastic filler particles and the tangled matrix. Three different types of filler surface are considered. The first type is a smooth spherical particle having no interaction with the polymer. The second type of particle is basically spherical but contains cavities or crevices into which sections of the polymer chain can enter. The third type of particle can form attachments with the neighboring polymer chains. These two surface modifications can occur separately or together. If both are present, their effect is additive.

In an unfilled elastomer under tension, the forces are extensive in the direction of the stress and compressive perpendicular to the stress. The forces are uniform throughout the sample except at the surface. When inelastic filler particles are present, the sections of tangle between adjacent filler particles in the plane perpendicular to the extension are compressed. The untangling in this region is repressed and further hinders the untangling in neighboring regions. This mechanism does not depend on any surface interaction between polymer and filler.

If the filler particles contain crevices, sections of the tangle may be constrained by the walls of the cavity. They

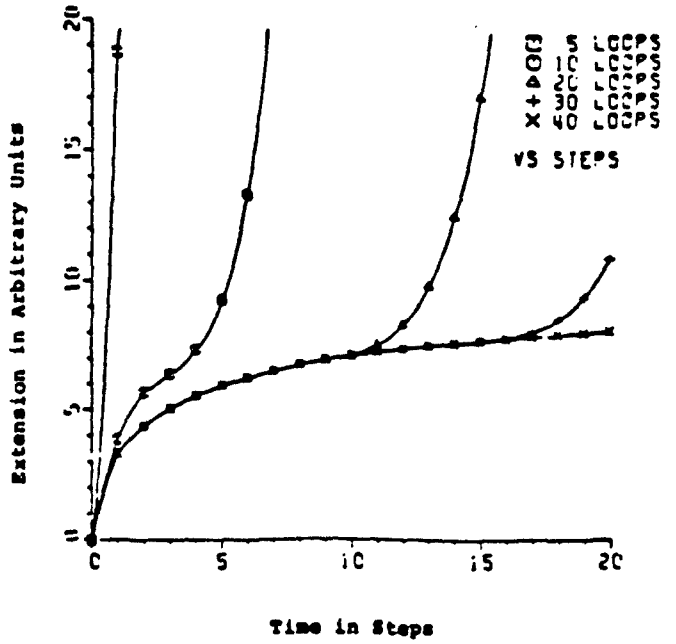

Figure 5-8. Calculated creep curves for monodisperse loop-entangled strands. Five cases of different length are shown. A step is the time unit corresponding to the Markov chain.

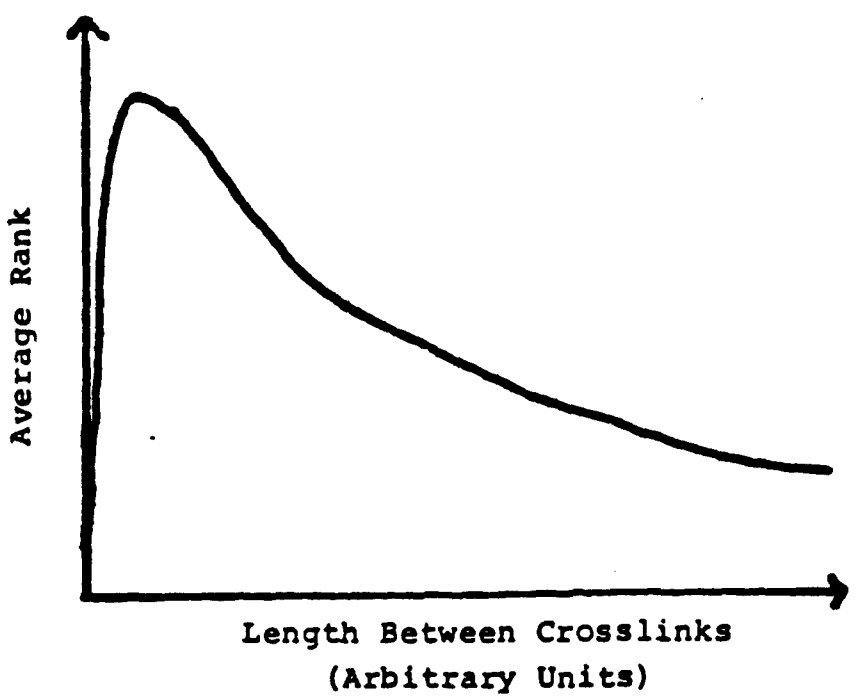

Figure 5-9. Calculated average rank as a function of length between crosslinks.

will tend to remain there and will lock any loops that they are entangled with, thus increasing the reinforcing effect of the filler.

Attractive forces between the surface of the filler and the polymer reduce the mobility of the loops adjacent to the filler surface and hinder untangling. Even weak attachments between polymer and filler inhibit the motion of the loops involved, thus preventing or greatly slowing their untangling. It is apparent with this model that the increase in strength in such a system is not directly dependent on the strength of these attachments in relation to the stress. To be effective, the attachments need only overcome the random motion of the polymer chain. The attachments will be effective to the extent that they inhibit the motion of the adsorbed loops. The response is controlled by the entanglement, not by the polymer-filler attachments. This inhibition increases with the number of attachments up to the limit at which all loops in contact with the filler surface are hindered.

Figure 5-10 shows the curves obtained by plotting the calculated reinforcement as a function of the fraction of the maximum loading for several values of the radius when the surface efficiency ratio of the particles is zero. Figure 5-11 shows the curves obtained for values of the surface efficiency ratio ranging from 0 to 1 for a radius of 0.01.

Decreasing particle size increases the reinforcement in this model. The curves obtained by plotting reinforcement as a function of filler loading show the maxima characteristically obtained in real systems. Increasing the surface activity ratio increases the reinforcement and also shifts the maximum reinforcement toward higher filler loadings. Beyond a critical value of the surface activity ratio, the curves showed no maximum as shown in Figure 5-12. The surface activity ratios actually attained in real systems are probably well below this critical level. The shift in the maximum is independent of particle size, at least for uniform spherical particles. For hexagonal packing, the plots of reinforcement as a function of loading show a maximum up to a surface efficiency ratio of 0.43.

5.3.4.4. Crystallization. Assume that crystallization begins with Loop A in Figure 5-13. Additional material for the growth of the crystal is freed by the relocation of Loops B and C. No relocations are required in parts far from the growing crystal. No center of mass motion is required in this model. The rate is controlled by the times required for sequential zero rank loop formation.

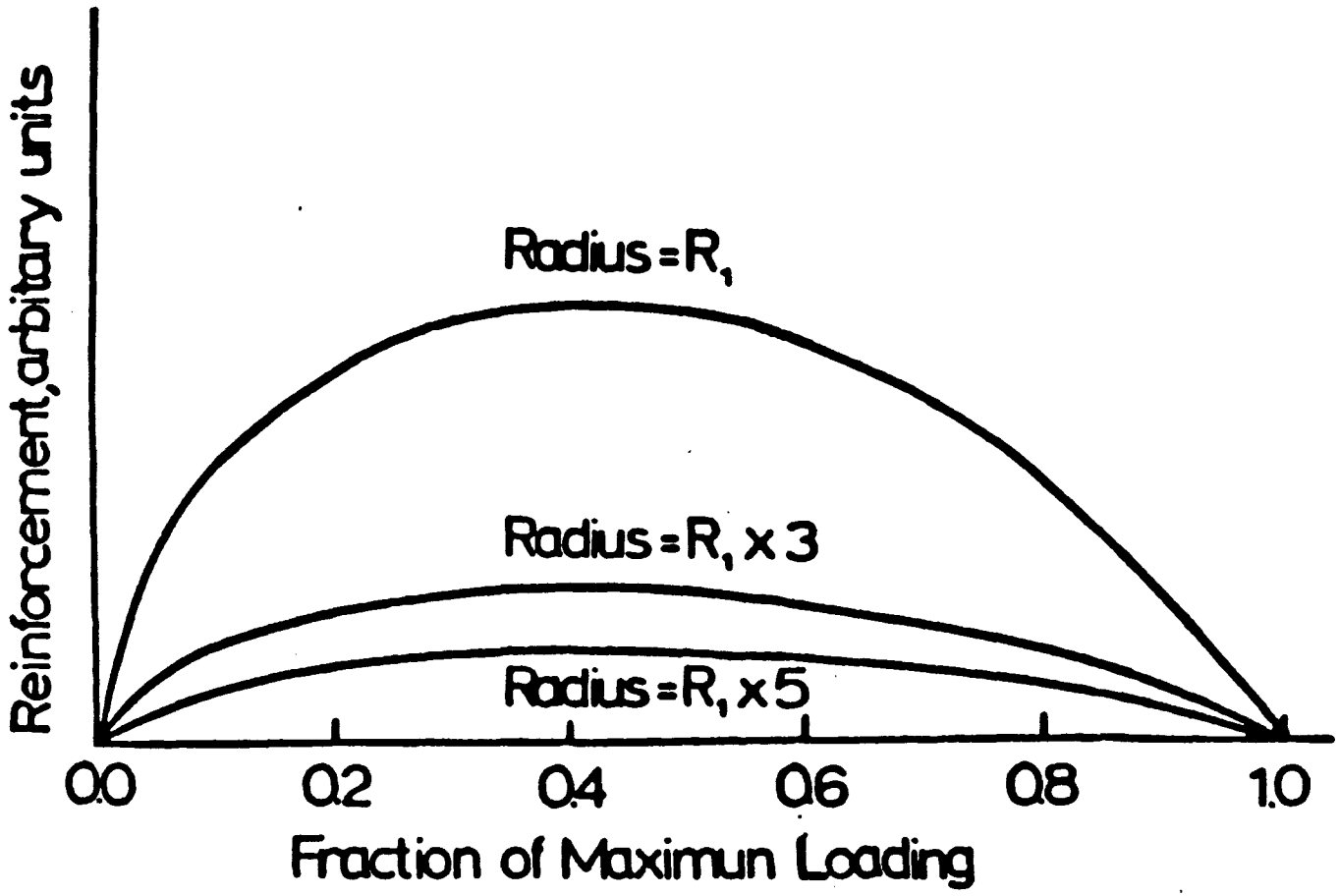

Figure 5-10. Calculated reinforcement in arbitrary units as a function of filler loading for spherical particles of different radius.

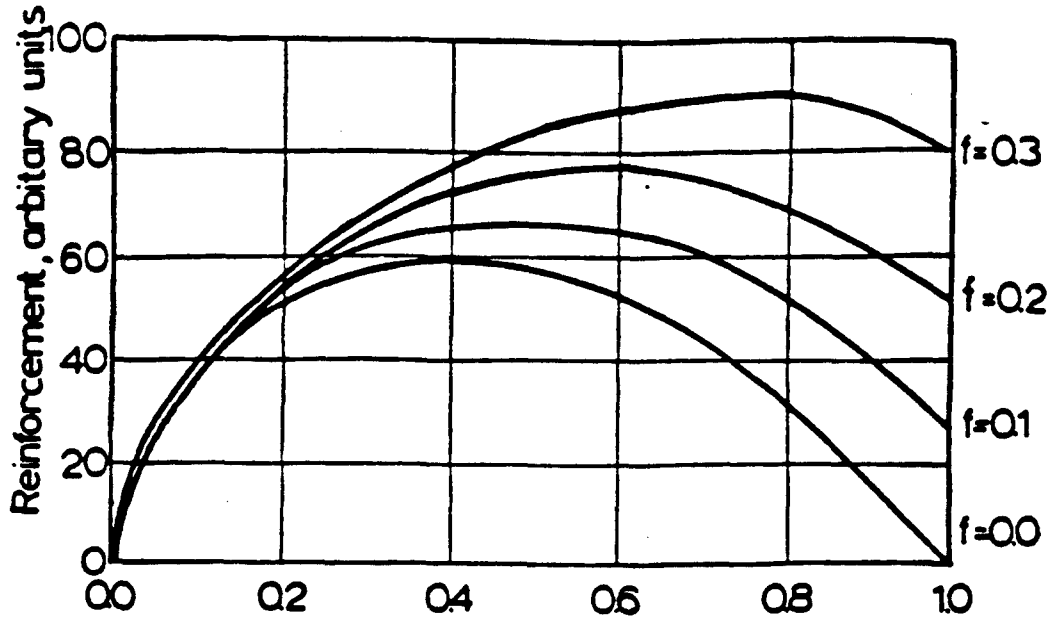

Figure 5-11. Calculated reinforcement as a function of filler loading for spherical particles of surface activity ratios of 0.0 to 0.3.

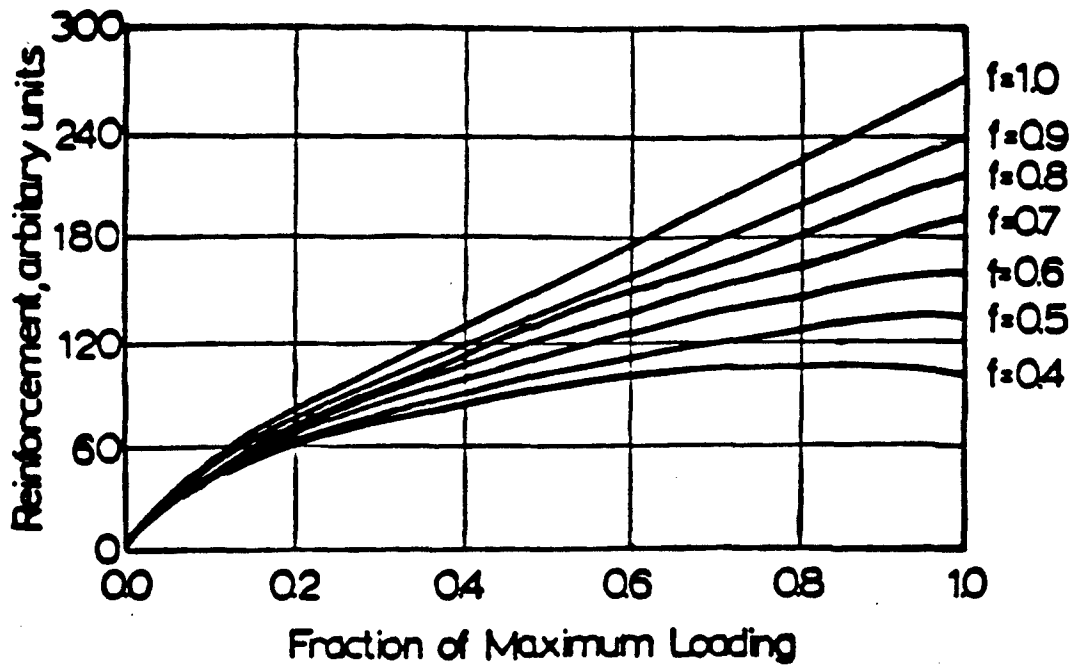

Figure 5-12. Calculated reinforcement as a function of filler loading for spherical particles of surface activity ratios of 0.4 to 1.0.

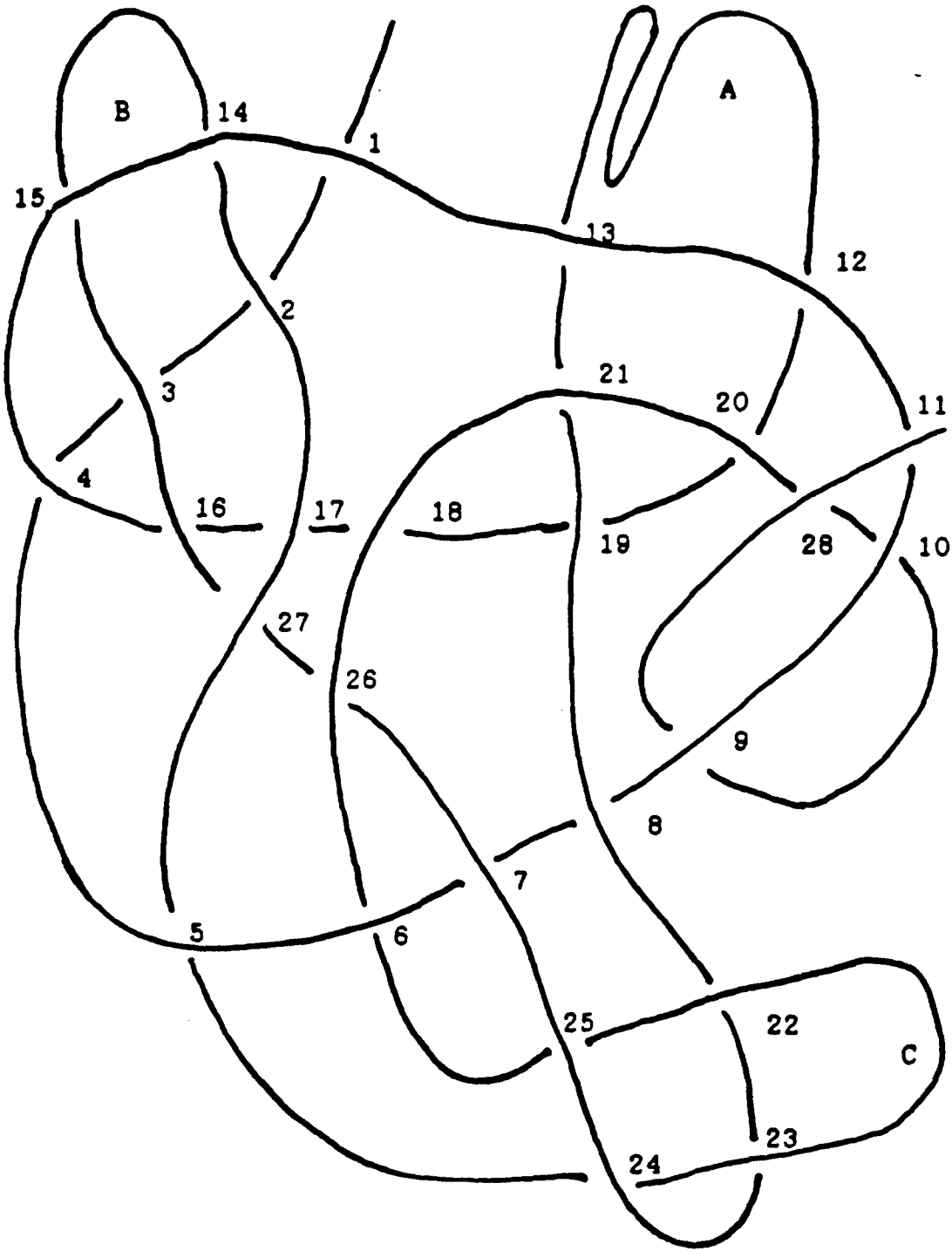

Figure 5-13. If crystallization begins with loop A, the relocation of loops B and C will free additional material for crystal growth.

Crystallization and crosslinking interact in a complex manner. Stress crystallization hinders the sections of chain involved in the crystal and thus acts in part as a temporary crosslink - the effect of which depends on the distribution at the moment of its formation. At the same time, crosslinking lowers the rate at which material can be fed into the crystal by decreasing the number of zero rank loops in the system. These interrelationships deserve close attention and will be studied further.

5.3.4.5. Polymer Welding by Loop Interaction. When two compatible polymer surfaces above the glass transition are brought into contact, loop interactions will occur between loops of different faces. As time passes, more interactions and interactions of higher order are formed. Since no motion of the whole chain or of chain ends is needed, this model applies equally to lightly crosslinked, branched or cyclic molecules.

5.3.4.6. Block Polymer Domain Formation. Differences in chain flexibility and mass per carbon atom will cause differences in the distribution of loop speeds for different polymers. This fact, in addition to factors of chemical compatibility, will make the probability of interaction with a like loop differ from that of interaction with an unlike loop for each species. These differences will vary with temperature. If the probability of interaction with a like loop is greater than that of interaction with an unlike loop for each species, domain formation is favored.

A thermoplastic elastomer has domains of glassy segments in a rubbery matrix. At the surface of the glassy domains some rubbery loops will be locked by glassy loops. Interactions of the type G = G = ... = R, where two or more glassy loops are found in the linking sequence leading to a rubbery loop, will tend to remain because of the low mobility of the glassy loops. The transition probabilities controlling the beginning of the sequence will not be affected by the lower compatibility elsewhere in the sequence. In addition to tying the domains together physically, this hindrance to the untangling of some rubbery loops will shift the equilibrium of the entanglement in the rubbery matrix as described in section 5.3.3.

A detailed discussion of these concepts is given in the doctoral dissertation of A. MacArthur entitled "A Loop Model of Polymer Entanglement", the University of Akron, 1985 [21].

5.4. The Chemical Behavior of Natural Rubber at the Temperatures of Track Pad Operation

5.4.1. Effect of Resin Components on Degradation of Guayule Rubber. All natural rubbers usually contain some long chain fatty acids or their esters. The individual effect of the four C_{18} fatty acids (stearic, oleic, linoleic and linolenic acid) present in the guayule resin on the degradation of GR has been investigated concurrently by stress-relaxation of radiation cured rubber networks and by gel permeation chromatography studies on the raw rubber in the temperature zone 70°C to 125°C. C_{18} unsaturated fatty acids enhance the degradation of rubber several fold. The rate of degradation follows the order: rubber < rubber + stearic acid < rubber + oleic acid < rubber + linoleic acid < rubber + linolenic acid. The thermal degradation is slower than the thermooxidative. The rate of degradation monotonically increased with the number of conjugated double bonds and is first order with respect to acid concentration. The activation energy for the chain scission for both thermal and thermooxidative degradation is 95 +/- 10 kJ/mole. The mechanism of degradation of GR in the presence of fatty acids is discussed.

GR containing a high concentration of its natural plant resin has poor oxidative stability. These resins are mainly mixtures of α-pinene, β-pinene, cadinene, linomene, sesquiterpene alcohol, partheniol, and fatty acids in different proportions. Recent studies[22,23] show that the effects of guayule resin on the degradation of HR are due to the presence of unsaturated fatty acids. The acids oxidize rapidly to form hydroperoxide and function as an initialtor in the degradation of the rubber. The relative percentages of fatty acids reported in guayule resin are: 6.9% palmitic acid, 5.6% stearic acid, 5.3% oleic acid, 65.1% linoleic acid, and 17.1% linolenic acid. Although HR and GR are identical in the backbone polymeric structure, cis 1,4 polyisoprene, the gel content and amount and type of non-rubber ingredients in HR are different from those of GR. How all of these non-rubber ingredients protect HR in storage is not clearly understood. Moreover, there is very little systematic investigation of the effect of the resins in the long-term storage of bulk GR. It is important to know these to predict the storage stability of GR. Hence a systematic study has been undertaken to examine the effect of individual components of the fatty acid resins on the degradation behavior of bulk GR.

The degradative effect of resin components on GR both in air and in a nitrogen atmosphere has been studied concurrently by stress relaxation of radiation-cured rubber and by following the average molecular weight of unvulcanized raw rubber after

degradation in the temperature zone 70°C to 125°C. In general, the rate of degradation is faster in air than in nitrogen atmosphere. The C_{18} unsaturated fatty acids enhance the degradation of rubber several fold compared to the corresponding saturated fatty acid, stearic acid. The rate of degradation caused by the fatty acids increases in the order linolenic acid > linoleic acid > oleic acid > stearic acid and is first order with repect to the acid concentration. This has been observed in both stress relaxation experiment and GPC studies. The effect of these acids on the degradation of rubber is directly proportional to the number of double bonds. The activation energy for both oxidative and thermal degradation has been found to be 95 +/- 10 kJ/mole., similar to that for the oxidation of HR. The mechanism of increased degrdation of rubber in the presence of unsaturated fatty acids in air and in nitrogen is believed to be due to stabilization of the free radicals through delocalization over more than three carbon atoms.

The details of this work are reported in i) S. Rampalli[24] M.S. Thesis (Polymer Science), University of Akron, and ii) A. K. Bhowmick, S. Rampalli, and D. McIntyre[25],

5.4.2. The Degradation of Guayule Rubber and the Effect of Resin Components on Degradation at High Temperature. GR containing high concentrations of its natural plant resins has very poor oxidative stability. In this study, the degradative effect of these individual resins both in air and nitrogen atmosphere has been studied concurrently by both thermal analysis of the unvulcanized raw rubber and stress relaxation of the vulcanized rubber. In general, the rate of degradation is faster in air than in nitrogen atmosphere. Random scission of main chain occurs rather than scission at the crosslink sites. The rate of degradation caused by the acids increases in the order, linolenic acid > linoleic acid > oleic acid > stearic acid. The activation energy for oxidative degradation has been found to be about 92 kJ/mol, similar to that for the oxidation of hevea natural rubber. the thermogravimetric analyses of raw GR and subsequent molecular weight determinations of the degraded rubber have been carried out with and without added resin components. The results suggest a mechanism of degradation for this material.

A detailed discussion of this work is given in i) the M. S. Thesis of S. Rampalli, the University of Akron, entitled "Studies on the Degradation of Guayule Rubber"[26] and ii) A. K. Bhowmick et. al.[27].

5.5. The Physical Behavior of SBR Rubber as a Function of Cyclic Stress and Static Deformation Experienced in Track Pads

5.5.1. Heat Build-Up of Bonded Rubber Blocks Due to Shear Cycling. Bonded rubber blocks are widely used in engineering applications. Their mechanical properties have been extensively studied both theoretically and experimentally. Fewer papers deal with side effects (i.e. heat build-up) related to repeated mechanical deformations.

In this study an attempt has been made to relate the damping to the heat build-up in bonded rubber blocks. The thermal properties such as specific heat and thermal diffusivity were measured. The specific heat decreases with increasing carbon black loading.

A finite difference method was used to predict both the temperature profile over the volume of the blocks and the temperature as a function of time after commencement of the dynamic deformations.

Viscoelastic materials dissipate energy during cyclic deformations. This dissipated energy is converted into heat which is not easily conducted away in a large object such as a bonded block. Therefore, energy dissipation gives rise to heat build-up inside the blocks. The high temperature build-up accelerates degradation, decomposition, or fatigue failure.[28,29]

Typical heat build-up problems of blocks in engineering practice are tires, pads of tank tracks, helicopter rotors, and solid propellants. Tormey and Britton[30] studied the effect of cyclic loading on solid propellant grain structures. They observed that the temperature rise softened the propellant and that part of the material flowed out of the motor after extended vibration.

To date, many papers deal with mechanical proerties, even though very few study the thermo-mechanical coupling of viscoelastic materials under cyclic vibrations. Those thermomechanical studies were limited to the Lockheed solid propellants[31-34] in a one-dimensional system with simplified approximation.

The purpose of this study was to broaden the scope to a three-dimensional system for crosslinked elastomer blocks under dynamic and static shear and to compare the experimental results to numerical simulations. It is possible to predict reasonably well the temperature increase inside bonded rubber blocks during cyclic deformations using a numerical analysis,

viscoelastic data of the compounds and measured surface temperatures.

Separate calculations to predict the temperature change of the plates would, of course, eliminate the need to monitor their temperatures.

An extension of this work to take into account dynamic experiments performed under load rather than position control would permit the prediction of thermal instabilities, i.e. a rapid increase of the temperature due to local reductions in the modulus which increase the strain amplitude and thus give rise to increased viscoelastic dissipation.

A detailed discussion of this work is given in the doctoral dissertation of D. C. Kong[35], the University of Akron, entitled "Heat build-up of Bonded Rubber Blocks Due to Shear Cycling."

5.5.2. The Influence of Static Deformations and Carbon Black Loading on the Dynamic Properties of Elastomers under Tension. The dynamic viscoelastic properties of both filled and unfilled polymers under static deformations have been the subject of several publications[36].

Meinecke and Maksin[37] investigated the dynamic viscoelastic properties of vulcanized SBR (Solprene-303) containing nearly spherical carbon black under combined static and sinusoidal tensile deformations. They found that under a constant dynamic amplitude, the plots of both the dynamic stress amplitude and the energy loss per cycle were linearly dependent on $1/\alpha^2$, where α is the static extension ratio, and that the regression lines intersected the origin. They also reported that the nearly spherical carbon black used in their study affected the static and dynamic properties of the rubber in a manner consistent with the hydrodynamic theory of Guth and Gold.[38]

In the present paper the influence of static tensile deformations upon the dynamic properties of a well vulcanized SBR, reinforced with different levels of a high structure N330 carbon black, was investigated. The work was carried out at a constant dynamic strain amplitude to avoid possible side effects such as may have affected the previous results. The samples were tested using a forced vibration technique at a constant frequency of 0.25 Hz and room temperature.

The dynamic properties of a carbon black filled SBR vulcanizate were measured as a function of static tensile deformations. The effect of the static deformations could be

explained with the help of geometrical considerations and that of the carbon black loading using either of two theories. One theory is based upon the concept of a strain amplification in the rubbery matrix between the rigid filler particles of aspect ratio f (the Guth theory)[39,40]. The value of f = 4.7 necessary to obtain agreement between theory and experiment is much higher than the values found from direct observation. The other theory is based upon the concept of occluded rubber volume within the elongated structure of the carbon black particles (the Medalia theory)[41,42]. The good fit between the data and this theory seems to support the concepts upon which this theory is based.

A detailed discussion of this work is given in the doctoral dissertation of M. I. Taftaf., the University of Akron, entitled "The Effects of Carbon Black Loading and Static Deformation upon the Dynamic Properties of Elastomers." [43]

5.5.3. The Influence of Static Deformations and Carbon Black Loading on the Dynamic Properties of Elastomers under Compression. Similar to the extensional case (section 5.5.2) the dynamic properties of bonded circular SBR rubber blocks, were determined as a function of static compressive strains and of carbon black loading. The static and dynamic viscoelastic results were obtained from two different methods of sample bondings. The rubber blocks were either bonded in the deformed state (i.e., the deformed blocks had cylindrical form) or in the undeformed state (i.e., the deformed block bulged).

The purpose of this work is to expand on the previous extensional investigation (section 5.5.2), to investigate the relationship between both the dynamic tension and compression properties with respect to static deformations, as well as the effects of carbon black loading.

The effects of static compressive upon the dynamic properties of SBR rubber, reinforced by high structure carbon black (N330) were investigated. Two different methods of bonding the rubber blocks to rigid plates were employed.

The dynamic modulus and the energy loss per cycle were explained (as in the extensional case) with the help of geometrical considerations.

Both Medalia's[44,45] occluded rubber concept and the hydrodynamic theory of Guth[46,47] were utilized to explain the effects of carbon black loading upon the static and dynamic experimental results.

A detailed discussion of this work is given in the doctoral dissertation of M. I. Taftaf., the University of Akron, entitled "The Effects of Carbon Black Loading and Static Deformation upon the Dynamic Properties of Elastomers." [48]

LIST OF REFERENCES

1. W. Y. Lin, C. C. Kuo and D. McIntyre, Bulletin of the American Physical Society, 29, 412, (1984)

2. P. J. Corish, in "Science and Technology of Rubber," F. R. Eirich, Ed., Academic Press, New York, (1978)

3. F. P. Warner, W. J. MacKnight, amd R. S. Stein, J. Polym. Sci., Polym. Phys. Ed. 15, 2113 (1977)

4. Technical literature on UBEPOL VCR, UBE Industries Ltd., Tokyo, (1980)

5. P. J. Corish, Plastics and Rubber, Materials and Application, 5, 109 (1980)

6. R. Bond, G. F. Morton, and L. H. Krol, Polymer, 25, 132 (1984)

7. H. J. Fabris, I. Glen Hargis, R. A. Livigni and S. L. Aggarwal, paper presented at Rubber Div., American Chemical Society Meeting, Houston, October, (1983)

8. W. Cooper and G. Vaughan, Polymer, 4, 329 (1963)

9. A. J. Carter, C. K. L. Davies and A. G. Thomas, paper presented at the First Italian-Polish Seminar on Multicomponent Polymeric Systems, Capri, Italy, Oct., (1979)

10. A. K. Bhowmick, C. C. Kuo, A. Manzur, A. MacArthur, and D. McIntyre, J. Macromol Sci.--Phys., B25(3), 283-306 (1986)

11. C. C. Kuo, "Properties of Crystalline-Rubbery Polymer Blends and Blocks with Differing Compatibility and Chain Stiffness" Ph. D. Dissertation (Polymer Science), The University of Akron, (1981)

12. A. K. Bhowmick, C. C. Kuo, A. Manzur, A. MacArthur and D. McIntyre, Spring Meeting, Rubber Division, A. C. S., Paper #59 (1984)

13. Portion of work for A. Manzur's doctoral dissertation

14. J. Cho, "Crystallization and Strain Birefringence of Uncrosslinked Natural Rubber as a Function of Molecular Weight and Gel Content," M.S. Thesis (Polymer Science), The Univ. of Akron, (1986)
15. H. W. Greensmith, Trans. I.R. I., 42, T267 (1966)
16. L. C. Bateman, Proceedings of a symposium of the International Rubber Group, Washington, D. C., (1962)
17. T. Hager, A. MacArthur, D. McIntyre, R. Seeger, Rubber Chem Technol., 52, 693 (1979)
18. ASTM D1278-76 and ASTM D2227-80
19. M. Oroz, "The Effect of Residual Plant Tissue and Minerals on the Properties of Natural Rubbers," M.S. Thesis (Polymer Science), University of Akron, (1983)
20. S. Kasemsuwam, "Characterization of Guayule Plant Residues and their Effect upon the Mechanical Properties of Rubber," M.S. Thesis (Polymer Science), The University of Akron, (1985)
21. A. MacArthur, "A Loop Model of Polymer Entanglement," Ph.D. Dissertation (Polymer Science), The University of Akron, (1985)
22. S. Rampalli, "Studies on the Degradation of Guayule Rubber," M.S. Thesis (Polymer Science), The University of Akron, (1984)
23. A. K. Bhowmick, S. Rampalli, and D. McIntyre, J. Appl. Polym. Sci., 30, 6, (1985)
24. R. W. Keller and H. L. Stephens, Rubber Chem. Technol., 55, 161 (1982)
25. R. W. Keller, D. S. Winkler and H. L. Stephens, Rubber Chem. Technol., 54, 115 (1981)
26. S. Rampalli, op. cit.
27. A. K. Bhowmick, S. Rampalli, K. Gallagher, R. Seeger, and D. McIntyre, J. Appl. Polym. Sci., (in press)
28. H. W. Greensmith, J. Appl. Polymer Sci., &, 993 (1963)
29. A. N. Gent and J. E. McGrath, J. Polymer Sci., A2, 1473 (1965)

30. J. F. Tormey and S. C. Britton, AIAA J, 1, 1763 (1963)

31. R. A. Schapery, AIAA J, 2, 1763 (1964)
32. R. A. Schapery, J. Appl. Mechanics, 32, 61, (1965)

33. R. A. Schapery, and D. E. Cantey, AIAA J, 4, 255 (1966)

34. N. C. Huang and D. E. Lee, J. Appl. Mechanics, 34, 127, (1967)

35. D. C. Kong, "Heat Build-up of Bonded Rubber Blocks Due to Shear Cycling," Ph. D. Dissertation (Polymer Science), The University of Akron, (1983)

36. A. I. Medalia, Rubber Chem. Tech., 51, 438 (1978)

37. E. A. Meinecke and S. Maksin, Rubber Chem. Tech., 54, 857 (1981)

38. E. Guth and O. Gold, Phys Rev., 53, 322 (1938)

39. E. Guth, Proc. Rubber Tech. Conf., 2nd (London), 353 (1948)

40. E. Guth, J. Appl. Phys., 16, 20 (1945)

41. A. I. Medalia, Rubber Chem. Tech., 45, 1171 (1972)

42. A. I. Medalia, Rubber Chem. Tech., 46, 877 (1973)

43. M. I. Taftaf, "The Effects of Carbon Black Loading and Static Deformation upon the Dynamic Properties of Elastomers," Ph. D. Dissertation (Polymer Science), The University of Akron, (1984)

44. E. Guth, Proc. Rubber Tech. Conf., 2nd (London), 353 (1948)

45. E. Guth, J. Appl. Phys., 16, 20 (1945)

46. A. I. Medalia, Rubber Chem. Tech., 45, 1171 (1972)

47. A. I. Medalia, Rubber Chem. Tech., 46, 877 (1973)

48. M. I. Taftaf, op. cit.

LIST OF ABBREVIATIONS, ACRONYMS AND SYMBOLS

Å	Angstroms
BR	Polybutadiene
C	Celsius
c-PI	Cis-polyisoprene
cis-BD	Cis-polybutadiene
DSC	Differential Scanning Calorimetry
GR	Guayule Rubber
HR	Hevea Rubber
LALLS	Low Angle Laser Light Scattering
MW	Molecular Weight
NR	Natural Rubber
SBR	Styrene-Butadiene Rubber
SIC	Strain Induced Crystallization
SMR-5	Standard Malaysian Rubber
t-PI	Trans-polyisoprene
Trans-BD	Trans-polybutadiene
vinyl-BD	Syndiotactic 1,2-Polybutadiene
WAXS	Wide Angle X-Ray Scattering

DISTRIBUTION LIST

	Copies
Commander U. S. Army Tank-Automotive Command ATTN: DRS7A-RCKT Warren, MI 48397-5000	3
Mr. Jacob Patt U. S. Army Tank-Automotive Command ATTN: DRS7A-RCKT Warren, MI 48397-5000	1
Mr. Billy Conley Office of Naval Research Resident Representative The Ohio State University Research Foundation 1314 Kinnear Road Columbus, OH 43212	1
Commander Defense Technical Information Center Bldg. 5, Cameron Station ATTN: DDAC Alexandria, VA 22314	12
Manager Defense Logistics Studies Information Exchange ATTN: AMXMC-D Fort Lee, VA 23801-6044	2
Commander U.S. Army Tank-Automotive Command ATTN: AMSTA-DDL Warren, MI 48397-5000	2
Commander U.S. Army Tank-Automotive Command ATTN: AMSTA-CF (Mr. Orlicki) Warren, MI 48397-5000	2